

Cadmium Selectively Induces MIP-2 and COX-2 Through PTEN-Mediated Akt Activation in RAW264.7 Cells

Yin-Yin Huang,^{*,1} Mi-Zhen Xia,^{†,1} Hua Wang,^{*,1} Xiao-Jing Liu,^{*,†} Yong-Fang Hu,^{*} Yuan-Hua Chen,^{*,†} Cheng Zhang,^{*} and De-Xiang Xu^{*,2}

^{*}Department of Toxicology, Anhui Medical University, Hefei, China; [†]Life Science College, Anhui Medical University, Hefei, China; and [‡]First Affiliated Hospital, Anhui Medical University, Hefei, China

¹These authors contributed equally to this work.

²To whom correspondence should be addressed at Department of Toxicology, Anhui Medical University, Hefei 230032, China. Tel: +86 551 65167923 E-mail: xudex@126.com.

Received September 18, 2013; accepted January 9, 2014

Increasing evidence demonstrates that cadmium (Cd) induces inflammation, but its mechanisms remain obscure. The present study showed that treatment with CdCl₂ selectively upregulates macrophage inflammatory protein (MIP)-2 and cyclooxygenase (COX)-2 in RAW264.7 cells. Concomitantly, Cd²⁺ markedly elevated the level of phosphorylated Akt in dose- and time-dependent manners. LY294002, a specific inhibitor of phosphatidylinositol 3-kinase (PI3K), blocked Cd²⁺-evoked Akt phosphorylation. Correspondingly, LY294002 significantly repressed Cd²⁺-induced upregulation of MIP-2 and COX-2 in RAW264.7 cells. Further experiments showed that treatment with Cd²⁺ significantly reduced the level of PTEN protein in RAW264.7 cells. MG132, a specific proteasome inhibitor, blocked Cd²⁺-induced reduction in PTEN protein as well as Akt phosphorylation, implicating the involvement of proteasome-mediated PTEN degradation. Of interest, Cd²⁺-induced degradation of PTEN protein appears to be associated with PTEN ubiquitination. N-acetylcysteine, a glutathione (GSH) precursor, blocked Cd²⁺-evoked PTEN degradation as well as Akt phosphorylation. By contrast, L-buthionine-S,R-sulfoximine, an inhibitor of cellular GSH synthesis, exacerbated Cd²⁺-induced PTEN degradation and Akt phosphorylation. Alpha-phenyl-N-tert-butyl nitron and vitamin C, two antioxidants, did not prevent from Cd²⁺-induced PTEN degradation and Akt phosphorylation. In conclusion, Cd²⁺ selectively induces MIP-2 and COX-2 through PTEN-mediated PI3K/Akt activation. Cellular GSH depletion mediates Cd²⁺-induced PTEN degradation and subsequent PI3K/Akt activation in macrophages.

Key words: cadmium; toxicity; inflammation; phosphatidylinositol 3-kinase (PI3K)/Akt.

Cadmium (Cd) is one of major occupational and environmental toxicants. Cd is frequently used in the process of electroplating, pigments, paints, welding, and Ni–Cd batteries, during which workers are exposed to Cd at significantly high levels (Beveridge *et al.*, 2010). The general population is also exposed to Cd via drinking water, contaminated food and cigarette smoking at a low level (Byrne *et al.*, 2009). Increasing evi-

dence has demonstrated that Cd induces inflammation. According to several *in vitro* reports, Cd²⁺ significantly increased the expression of cyclooxygenase (COX)-2 and the production of prostaglandin E₂ in neonatal mouse calvaria and primary mouse osteoblastic cells (Miyahara *et al.*, 2004; Romare and Lundholm, 1999). An *in vivo* study showed that oral CdCl₂ exposure significantly increased macrophage inflammatory protein (MIP)-2 mRNA in the proximal intestine of mice (Zhao *et al.*, 2006). Moreover, treatment with Cd²⁺ induces interleukin (IL)-8 in human intestinal Caco-2 cells and airway epithelial cells (Cormet-Boyaka *et al.*, 2012; Hyun *et al.*, 2007). A recent study found that culture with CdCl₂ stimulated the release of tumor necrosis factor (TNF)- α in primary human monocytes (Haase *et al.*, 2010). Nevertheless, the mechanisms of Cd-evoked inflammation remain to be determined.

PTEN (phosphatase and tensin homolog deleted on chromosome 10) is one of the most frequently mutated tumor suppressors (Song *et al.*, 2012). The characterized function of PTEN is its lipid phosphatase activity, which antagonizes the phosphoinositide 3-kinase (PI3K) and subsequent activation of protein kinase B/Akt signaling (Hollander *et al.*, 2011). Although the function of PTEN has been extensively studied in the field of cancer research, increasing evidence has elucidated the function of PTEN as a negative regulator in the immune system (Harris *et al.*, 2008). An earlier study showed that T-cell-specific loss of PTEN led to increased PI3K-dependent signaling events, such as Akt phosphorylation and increased secretion of inflammatory cytokines (Suzuki *et al.*, 2001). By contrast, administration of adenoviruses carrying PTEN cDNA or PI3K inhibitors downregulates the expression of vascular endothelial growth factor in allergen-induced airway inflammation (Lee *et al.*, 2006). Indeed, Cd causes rapid activation of Akt signaling, a downstream target of PTEN, in human breast cancer cells (Liu *et al.*, 2008). According to several recent reports, Cd induces activation of PI3K/Akt signaling and malignant transformation of human bronchial epithelial cells (Jing *et al.*, 2012; Son *et al.*,

2012). Thus, we hypothesize that PTEN-mediated PI3K/Akt signaling also plays an important role on Cd²⁺-evoked inflammation.

In the present study, we showed that the expression of MIP-2 and COX-2 was significantly elevated in Cd²⁺-treated RAW264.7 cells. We demonstrate for the first time that Cd²⁺-induced upregulation of MIP-2 and COX-2 is associated with the activation of PI3K/Akt signaling in RAW264.7 cells. Moreover, proteasome-mediated PTEN degradation is involved in the activation of PI3K/Akt signaling in Cd²⁺-stimulated RAW264.7 cells. Finally, cellular glutathione (GSH) depletion contributes, at least partially, to Cd²⁺-induced PTEN degradation and subsequent activation of PI3K/Akt signaling in RAW264.7 cells.

MATERIALS AND METHODS

Chemicals and reagents. Cadmium chloride (CdCl₂), N-acetylcysteine (NAC), alpha-phenyl-N-tert-butyl nitron (PBN), LY294002, MG132, buthionine sulfoximine (BSO), and vitamin C were purchased from Sigma Chemical Co. (St. Louis, MO). Antibodies against COX-2 and β-actin were from Santa Cruz Biotechnologies, Inc. (Santa Cruz, CA). Akt, phosphor-Akt (pAkt), and PTEN antibodies were from Cell Signaling Technology (Beverly, MA). Chemiluminescence (ECL) detection kit was from Pierce Biotechnology (Rockford, IL). TRIzol reagent was from Molecular Research Center, Inc (Cincinnati, OH). RNase-free DNase, and real time (RT) and Polymerase Chain Reaction (PCR) kits were from Promega Corporation (Madison, WI). All the other reagents were from Sigma or as indicated in the specified methods.

Cell culture and treatments. RAW264.7 cells, a rodent macrophage cell line, were grown in Nunc flasks in Dulbecco's modified Eagle's medium supplemented with 100 U/ml of penicillin, 100 μg/ml streptomycin, 10 mm 4-(2-hydroxyethyl) piperazine-1-erhaesulfonic acid, 2mM L-glutamine, 0.2% NaHCO₃, and 10% [v/v] heat-inactivated fetal calf serum in a humidified chamber with 5% CO₂/95% air at 37°C. For measurement of cytotoxicity, RAW264.7 cells (1 × 10³ ~1 × 10⁴ cells/ml) were grown in 96-well plates for 24 h. The cells were then incubated with different concentrations of CdCl₂ (0, 6.25, 12.5, 25, and 50 μM) for different times (0, 4, 8, 16, and 24 h). Cell viability was detected using the colorimetric 3-(4,5-dimethyl-2-thiazolyl)-2,5-diphenyl 1-2H-tetrazoliumbromide (MTT) assay. For detection of cytokines/chemokines and inflammatory signaling, RAW264.7 cells were seeded into 6-well culture plates at a density of 5 × 10⁵ cells/well and incubated for at least 12 h to allow them to adhere to the plates. After washing three times with medium, the cells were incubated with different concentrations of CdCl₂ (0, 6.25, 12.5, 25, and 50 μM) for different times (0, 4, 8, or 16 h). The cells were washed with chilled phosphate buffer

solution (PBS) for three times and then harvested for real-time RT-PCR, Western blot, and immunoprecipitation.

Isolation of total RNA and real-time RT-PCR. Total RNA was extracted using TRI reagent. RNase-free DNase-treated total RNA (1.0 μg) was reverse-transcribed with Avian Myeloblastosis Virus (Pregmega Corporation, Madison, WI). Real-time RT-PCR was performed with a LightCycler 480 SYBR Green I kit (Roche Diagnostics GmbH, Mannheim, Germany) using gene-specific primers as listed in Table 1. The amplification reactions were carried out on a LightCycler 480 Instrument (Roche Diagnostics GmbH) with an initial hold step (95°C for 5 min) and 50 cycles of a three-step PCR (95°C for 15 s, 60°C for 15 s, and 72°C for 30 s). The comparative C_T-method was used to determine the amount of target, normalized to an endogenous reference (gapdh) and relative to a calibrator (2^{-ΔΔC_T}) using the Lightcycler 480 software (Roche, version 1.5.0). All RT-PCR experiments were performed in triplicate.

Immunoblot. To prepare cell lysates, cells were washed three times with ice-cold PBS and lysed by incubating for 30 min on ice with 200 μl of lysis buffer (50mM Tris-HCl, pH 7.4, 150mM NaCl, 1mM Ethylene Diamine Tetraacetic Acid, 1% Triton X-100, 1% sodium deoxycholate, 0.1% sodium dodecylsulfate, 1mM phenylmethylsulfonyl fluoride) supplemented with a cocktail of protease inhibitors (Roche, Indianapolis, IN). The cell lysates were centrifuged at 10,000 × g for 10 min to remove insoluble material. Protein concentrations were determined with the bicinchoninic acid protein assay reagents (Pierce Biotechnology) according to the manufacturer's instructions. For immunoblots, same amount of protein (40~80 μg) was separated electrophoretically by SDS-polyacrylamide gel electrophoresis. The protein was transferred to a polyvinylidene fluoride membrane by electroblotting. The membranes were incubated for 2 h with the following antibodies (1:1000 dilution): Akt, pAkt, PTEN, and COX-2. β-actin was used as a loading control. After washes in DPBS containing 0.05% Tween-20 four times for 10 min each, the membranes were incubated with goat antirabbit IgG or goat antimouse antibody for 2 h. The membranes were then washed for four times in DPBS containing 0.05% Tween-20 for 10 min each, followed by signal development using an ECL detection kit.

Immunoprecipitation. RAW264.7 cells treated with different concentrations of CdCl₂ were lysed with Radio Immunoprecipitation Assay (RIPA) buffer (1% Nonidet P-40, 0.5% sodium deoxycholate, and 0.1% SDS in phosphate-buffered saline, pH 7.4) containing 0.1mM vanadyl sulfate and protease inhibitors (0.5 mg/ml aprotinin, 0.5 mg/ml trans-epoxy succinyl-L-leucylamido-(4-guanidino)butane (E-64), 0.5 mg/ml pepstatin, 0.5 mg/ml bestatin, and 10 mg/ml chymostatin, and 0.1 ng/ml leupeptin). Cell lysates (300 μg) were precleared with protein A-agarose and then incubated with agarose-conjugated PTEN antibody (Santa Cruz Biotechnology, Inc.,) at 4°C overnight.

TABLE 1
Primers for Real-time RT-PCR

Genes	Sequences	Sizes (bp)
<i>gapdh</i>	Forward: 5'- ACCCCAGCAAGGACACTGAGCAAG -3' Reverse: 5'- GGCCCTCCTGTTATTATGGGGGT -3'	109
<i>TNF-α</i>	Forward: 5'- CCCTCCTGGCCAACGGCATG -3' Reverse: 5'- TCGGGGCAGCCTTGTCCTT -3'	109
<i>IL-1β</i>	Forward: 5'- GCCTCGTGCTGTCGGACCCATAT -3' Reverse: 5'- TCCTTTGAGGCCCAAGGCCACA -3'	143
<i>IL-6</i>	Forward: 5'- AGACAAAGCCAGAGTCCTTCAGAGA -3' Reverse: 5'- GCCACTCCTTCTGTGACTCCAGC -3'	146
<i>MCP-1</i>	Forward: 5'- GGCTGGAGAGCTACAAGAGG -3' Reverse: 5'-GGTCAGCACAGACCTCTCTC -3'	93
<i>MIP-2</i>	Forward: 5'- TTGCCTTGACCCTGAAGCCCC -3' Reverse: 5'- GGCACATCAGGTACGATCCAGGC -3'	175
<i>MIP-1</i>		
<i>IL-10</i>	Forward: 5'- GCTCTAGAGCTGCGGACTGC -3' Reverse: 5'- TGCTTCTCTGCTGGGCATCA -3'	183
<i>iNOS</i>	Forward: 5'- GCTCGTTTGCCACGGACGA -3' Reverse: 5'- AAGGCAGCGGGCACATGCAA -3'	146
<i>COX-2</i>	Forward: 5'- GGGCTCAGCCAGGCAGCAAAT -3' Reverse: 5'- GCACTGTGTTGGGGTGGGCT -3'	187

The precipitates were washed with cold RIPA buffer before immunoblotting using a murine monoclonal ubiquitin antibody (Cascade Bioscience, Winchester, MA).

Statistical analysis. Quantified data were expressed as means \pm SEM at each point. ANOVA and the Student–Newmann–Keuls *post hoc* test were used to determine differences between the treated cells and the control. Differences were considered significant only for $P < 0.05$.

RESULTS

Cd²⁺-Induced Cytotoxicity in RAW264.7 Cells

Cd^{2+} -induced cytotoxicity in RAW264.7 cells was primarily evaluated using the MTT assay. In an 8-h-incubation protocol, all concentrations of $CdCl_2$ (6.25, 12.5, 25.0, and 50 μ M) had only a slight cytotoxicity in RAW264.7 cells (Fig. 1). From 12.5 to 50 μ M, cell viability was markedly decreased at 16 h after incubation with $CdCl_2$ in a concentration-dependent manner. At 24 h after incubation with $CdCl_2$, even a low concentration of $CdCl_2$ (6.25 μ M) led to a significant reduction in cell viability ($P < 0.01$).

Cd²⁺ Selectively Upregulates MIP-2 and COX-2 in RAW264.7 Cells

The effects of Cd^{2+} on the expression of cytokines/chemokines were analyzed in RAW264.7 cells. As cell viability was markedly decreased at 16 h after incubation, the expression of cytokines/chemokines was measured at 4 and 8 h after $CdCl_2$. As shown in Figure 2A, mRNA level of $TNF-\alpha$ was significantly decreased. Of interest, Cd^{2+} had no effect on the expression of $IL-1\beta$ and $IL-6$ in

RAW264.7 cells (Figs. 2B and C). The effects of Cd^{2+} on the expression of chemokines are presented in Figures 2D–F. Although Cd^{2+} caused a slight reduction in mRNA level of $MCP-1$, a chemokine (Fig. 2D), mRNA level of $MIP-2$, another chemokine, was increased by more than 150 folds 4 h after $CdCl_2$ and about 300 folds 8 h after $CdCl_2$ (Fig. 2E). As shown in Figure 2F, Cd^{2+} had no effect on the expression of $MIP-1$ in RAW264.7 cells. In addition, Cd^{2+} did not affect the expression of $IL-10$ in RAW264.7 cells (Fig. 2G). The effects of Cd^{2+} on $iNOS$ and $COX-2$ in RAW264.7 cells are presented in Figures 2H and I. Although Cd^{2+} had no effect on the expression of $iNOS$ (Fig. 2H), $COX-2$ mRNA was persistently upregulated in Cd^{2+} -treated RAW264.7 cells (Fig. 2I). We then analyzed the effects of different doses of Cd^{2+} on the expression of cytokines/chemokines in RAW264.7 cells. As shown in Figure 2J, Cd^{2+} downregulated mRNA level of $TNF-\alpha$ in a dose-dependent manner. Cd^{2+} had no effect on the expression of $IL-1\beta$ and $IL-6$ in RAW264.7 cells (Figs. 2K and L). As expected, Cd^{2+} caused a slight reduction in mRNA level of $MCP-1$ in high dose group (Fig. 2M). Although Cd^{2+} had no effect on the expression on MIP (Fig. 2O), Cd^{2+} upregulated the expression of $MIP-2$ in a dose-dependent manner (Fig. 2N). The effects of different doses of Cd^{2+} on $IL-10$, $iNOS$, and $COX-2$ were presented in Figures 2P–R. Although Cd^{2+} had no effect on the expression of $IL-10$ and $iNOS$ (Figs. 2P and Q), Cd^{2+} upregulated the expression of $COX-2$ in a dose-dependent manner (Fig. 2R). In the present study, we also measured the expression of inflammatory cytokines/chemotokines in RAW264.7 cells incubated with low concentration of $CdCl_2$ (6.25 μ M) for 16 h. As Supplementary figure 1, the expression of $TNF-\alpha$ was significantly downregulated in RAW264.7 cells incubated with low concentration of $CdCl_2$ (6.25 μ M) for 16

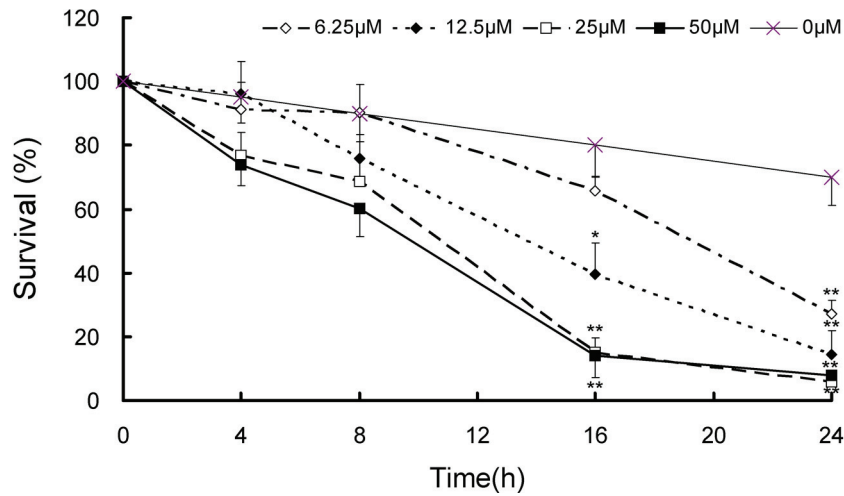


FIG. 1. Cd^{2+} -induced cytotoxicity. RAW264.7 cells were then preincubated with different concentrations of CdCl_2 (0, 6.25, 12.5, 25, and 50 μM) for different times (0, 4, 8, 16, and 24 h). Cell viability was detected using MTT assay. Data were expressed as means \pm SEM of six samples. * $P < 0.05$ and ** $P < 0.01$ as compared with control group.

h. Of interest, the expression of IL-10 in RAW264.7 cells was slightly upregulated 16 h after incubation with 6.25 μM of CdCl_2 (Supplementary figure 7). Incubation with low concentration of Cd^{2+} had no effect on IL-1 β , IL-6, MCP-1, MIP-2, MIP-1, iNOS, and COX-2 (Supplementary figures 1–6, 8, and 9).

PI3K/Akt Activation Is Involved in Cd^{2+} -Induced Upregulation of MIP-2 and COX-2 in RAW264.7 Cells

To investigate whether PI3K/Akt signaling is involved in Cd^{2+} -induced upregulation of MIP-2 and COX-2, pAkt/Akt was measured in Cd^{2+} -stimulated RAW264.7 cells. As shown in Figures 3A and B, the level of pAkt was markedly increased in Cd^{2+} -treated RAW264.7 cells in a time- and dose-dependent manner. The effects of LY294002, a specific inhibitor of PI3K, on Cd^{2+} -induced upregulation of MIP-2 and COX-2 were analyzed. As expected, LY294002 almost completely inhibited Cd^{2+} -induced Akt phosphorylation in RAW264.7 cells (Fig. 3C). Correspondingly, LY294002 obviously inhibited Cd^{2+} -induced upregulation of MIP-2 and COX-2 mRNA (Figs. 3D and E). In addition, LY294002 significantly attenuated Cd^{2+} -induced elevation of COX-2 protein in RAW264.7 cells (Fig. 3F).

Proteasome-Mediated PTEN Degradation Contributes To PI3K/Akt Activation In Cd^{2+} -Stimulated RAW264.7 Cells

The effects of Cd^{2+} on the level of PTEN protein in RAW264.7 cells are presented in Figure 4. As shown in Figures 4A and C, the level of PTEN protein was significantly reduced in Cd^{2+} -stimulated RAW264.7 cells in a dose-dependent manner. Further analysis showed that the level of PTEN protein was reduced by about 80% in 8 h after CdCl_2 (Figs. 4B and D). The effects of MG132, a specific inhibitor of pro-

teasome, on Cd^{2+} -induced reduction in PTEN protein were then investigated. Of interest, MG132 blocked Cd^{2+} -induced reduction in PTEN protein in RAW264.7 cells (Figs. 5A and B). Concomitantly, MG132 significantly attenuated Cd^{2+} -induced Akt phosphorylation (Figs. 5C and D). To investigate the mechanism of reduction in PTEN protein in Cd^{2+} -stimulated macrophages, ubiquitination of PTEN protein was then analyzed using IP. Although total PTEN protein was significantly decreased in Cd^{2+} -stimulated RAW264.7 cells, the level of ubiquitinated PTEN, which was partially degraded, was increased in Cd^{2+} -stimulated RAW264.7 cells in a dose-dependent manner (Fig. 5E). Finally, the expression of PTEN mRNA was investigated in Cd^{2+} -stimulated macrophages. Of interest, Cd^{2+} slightly downregulated the expression of PTEN mRNA in RAW264.7 cells (Fig. 5F).

Cellular GSH Depletion Is Involved In Cd^{2+} -Induced PTEN Degradation And Akt Activation In RAW264.7 Cells

The effects of Cd^{2+} on cellular GSH content in RAW264.7 cells were analyzed. Consistent with reduction in PTEN, cellular GSH content was significantly decreased in Cd^{2+} -stimulated RAW264.7 cells in a time-dependent manner (Fig. 6A). Interestingly, NAC, a GSH precursor, blocked Cd^{2+} -induced PTEN degradation in RAW264.7 cells (Figs. 6B and C). In addition, NAC blocked Cd^{2+} -induced Akt phosphorylation in RAW264.7 cells (Figs. 6D and E). By contrast, BSO, an inhibitor of cellular GSH synthesis, exacerbated Cd^{2+} -induced PTEN degradation in RAW264.7 cells (Figs. 6F and G). In addition, BSO aggravated Cd^{2+} -induced Akt phosphorylation in RAW264.7 cells (Figs. 6H and I).

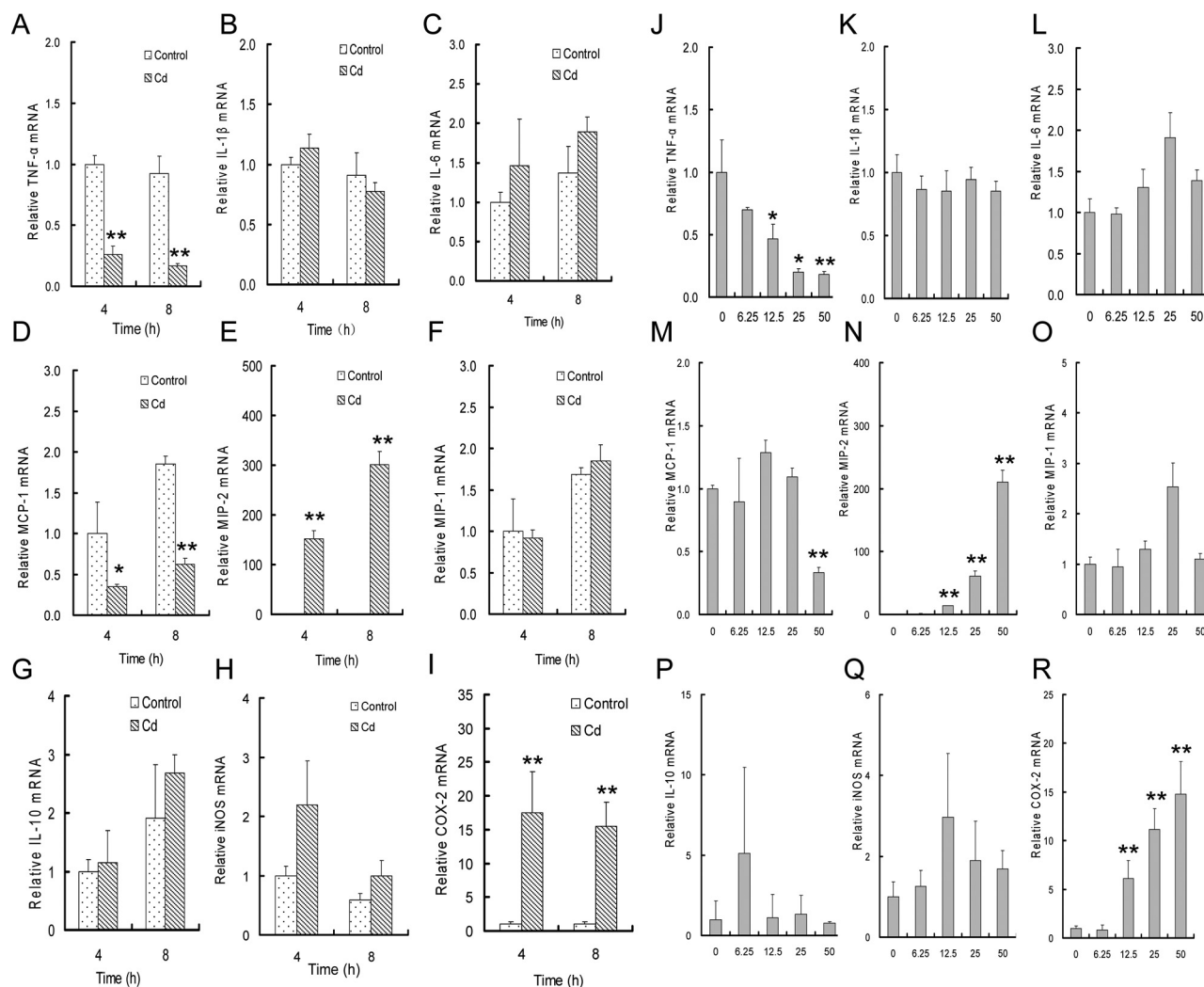


FIG. 2. Cd^{2+} selectively regulates the expression of inflammatory cytokines, chemokines, iNOS, and COX-2 in a dose-dependent manner. (A)–(I) RAW264.7 cells were incubated with CdCl_2 ($50.0\mu\text{M}$). The expression of inflammatory cytokines, chemokines, iNOS, and COX-2 was measured using real-time RT-PCR at 4 and 8 h after CdCl_2 . (A) TNF- α , (B) IL-1 β , (C) IL-6, (D) MCP-1, (E) MIP-2, (F) MIP-1, (G) IL-10, (H) iNOS, and (I) COX-2. (J)–(R) RAW264.7 cells were incubated with different concentrations of CdCl_2 (0, 6.25, 12.5, 25, or $50.0\mu\text{M}$). The expression of inflammatory cytokines, chemokines, iNOS, and COX-2 was measured using real-time RT-PCR at 8 h after CdCl_2 . (J) TNF- α , (K) IL-1 β , (L) IL-6, (M) MCP-1, (N) MIP-2, (O) MIP-1, (P) IL-10, (Q) iNOS, and (R) COX-2. Data were expressed as means \pm SEM of six samples. * $P < 0.05$ and ** $P < 0.01$ as compared with control group.

Antioxidants Do Not Affect Cd^{2+} -Induced PTEN Degradation And Akt Activation In RAW264.7 Cells

The effects of PBN, a free radical scavenger, on Cd^{2+} -induced PTEN degradation and Akt phosphorylation were analyzed. As shown in Figures 7A and B, PBN had little effect on Cd^{2+} -induced PTEN degradation in RAW264.7 cells. In addition, PBN did not affect Cd^{2+} -induced Akt phosphorylation in RAW264.7 cells (Figs. 7C and D). The effects of vitamin C, an antioxidant, on Cd^{2+} -induced PTEN degradation and Akt phosphorylation were then analyzed. Unexpectedly, vitamin C exacerbated Cd^{2+} -induced PTEN degradation in RAW264.7 cells (Figs. 7E and F). In addition, vitamin C aggravated Cd^{2+} -

induced Akt phosphorylation in RAW264.7 cells (Figs. 7G and H).

PI3K Inhibitor Partially Inhibited Cd^{2+} -Induced PTEN Degradation In RAW264.7 Cells

To investigate the influence of the PI3K/Akt signaling on Cd^{2+} -induced PTEN degradation, the effects of LY294002, a specific inhibitor of PI3K, on Cd^{2+} -induced reduction of PTEN protein were analyzed. As shown in Figure 8, the level of PTEN protein was significantly decreased in Cd^{2+} -stimulated RAW264.7 cells. Of interest, treatment with LY294002 partially attenuated Cd^{2+} -induced reduction of PTEN in RAW264.7 cells.

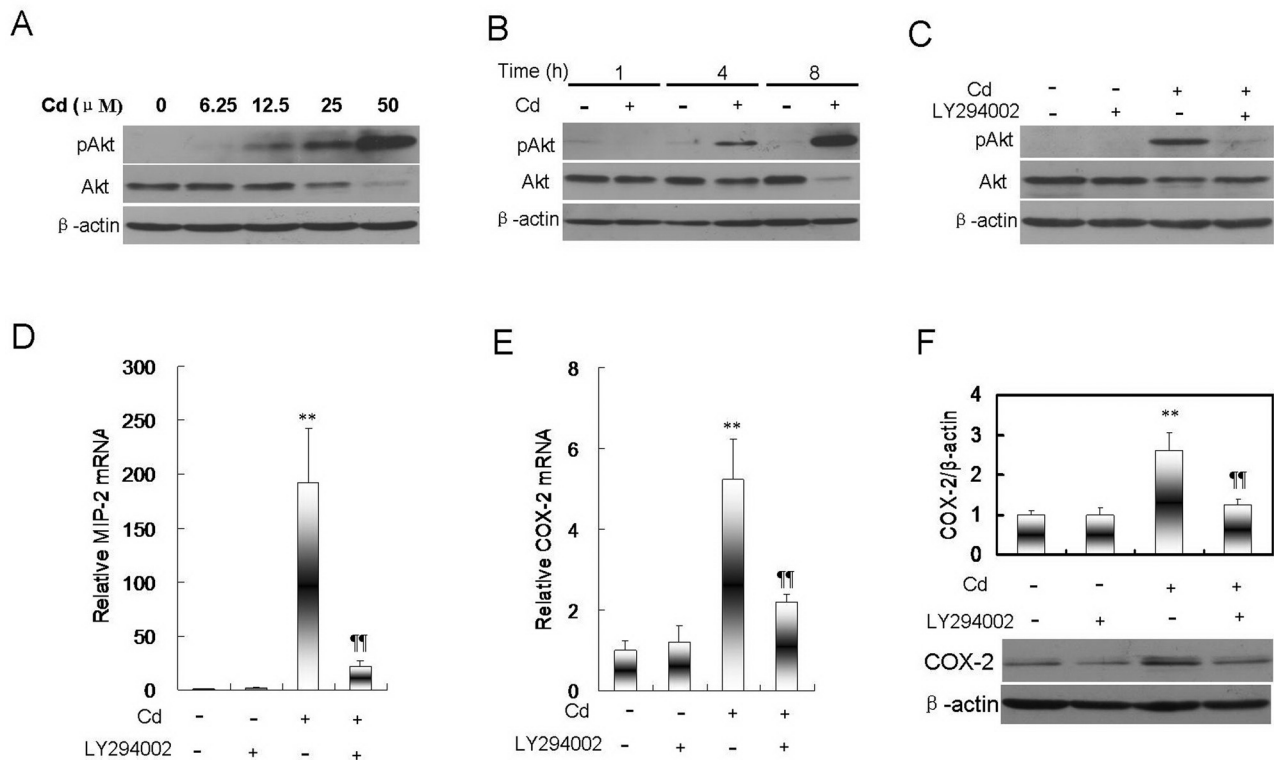


FIG. 3. Akt activation is involved in Cd²⁺-induced upregulation of MIP-2 and COX-2 in rodent macrophages. (A) RAW264.7 cells were incubated with different concentrations of CdCl₂ (0, 6.25, 12.5, 25, and 50.0 μM). Akt and pAkt were measured using Western blot at 8 h after CdCl₂. (B) RAW264.7 cells were incubated with CdCl₂ (50.0 μM). Akt and pAkt were measured using Western blot at 1, 4, and 8 h after CdCl₂. (C)–(F) RAW264.7 cells were incubated with CdCl₂ (50.0 μM) in the absence or presence of LY294002 (50.0 μM). (C) Akt and pAkt were measured using Western blot at 8 h after CdCl₂. (D) MIP-2 and (E) COX-2 mRNA was determined using real-time RT-PCR at 8 h after CdCl₂. (F) COX-2 protein was measured using Western blot at 8 h after CdCl₂. Data were expressed as means ± SEM of six samples. ***P* < 0.01 as compared with control group. ***P* < 0.01 as compared with CdCl₂ group.

DISCUSSION

The present study showed that treatment with CdCl₂ caused a significant elevation of COX-2 expression in macrophages in a dose-dependent manner. This result is in agreement with an earlier report (Seok *et al.*, 2006), in which Cd stimulates PGE₂ release accompanied by increase of COX-2 expression in cerebrovascular endothelial cells. A recent study has demonstrated that Cd²⁺ differentially regulates the expression of cytokines/chemokines in different types of cells (Lag *et al.*, 2010). The present study found that the expression of TNF-α and MCP-1 was downregulated after exposure to Cd²⁺ for 4–8 h, whereas Cd²⁺ did not affect the expression of IL-1β and IL-6 in macrophages. Of interest, the expression of MIP-2, a functional analogue of human IL-8, was upregulated by 150–300 folds in Cd²⁺-stimulated macrophages. These results suggest that Cd²⁺ selectively regulates cytokines/chemokines in macrophages. MIP-2/IL-8 may be important in governing the Cd²⁺-induced inflammatory responses.

The PI3K/Akt signaling is one of the most important signaling cascades that regulate inflammatory genes (Foster *et al.*, 2012). Indeed, the present study showed that the level of

phosphorylated Akt was markedly increased in Cd²⁺-treated macrophages, indicating that the PI3K/Akt signaling was activated by Cd²⁺. Increasing evidence indicates that COX-2 is a downstream target of PI3K/Akt signaling (Chen *et al.*, 2009; Rodriguez-Barbero *et al.*, 2006). The present study showed that LY294002, a specific inhibitor of PI3K, significantly attenuated Cd²⁺-induced upregulation of COX-2 mRNA in macrophages. In addition, LY294002 significantly attenuated Cd²⁺-induced elevation of COX-2 protein in macrophages. An earlier study found that oxidized low-density lipoprotein upregulated the expression of MIP-2 through activating PI3K/Akt signaling in macrophages (Miller *et al.*, 2005). The present study showed that Cd²⁺-induced upregulation of MIP-2 was blocked by LY294002. These results suggest that the PI3K/Akt signaling contributes, at least partially, to Cd²⁺-induced upregulation of MIP-2 and COX-2 in macrophages.

Increasing evidence demonstrates that PTEN negatively regulates PI3K signaling and subsequent Akt phosphorylation (Hollander *et al.*, 2011). To investigate the role of PTEN on Cd²⁺-induced Akt phosphorylation, the present study examined Cd²⁺-induced regulation of PTEN protein in macrophages. As expected, treatment with Cd²⁺ caused an obvious reduction in

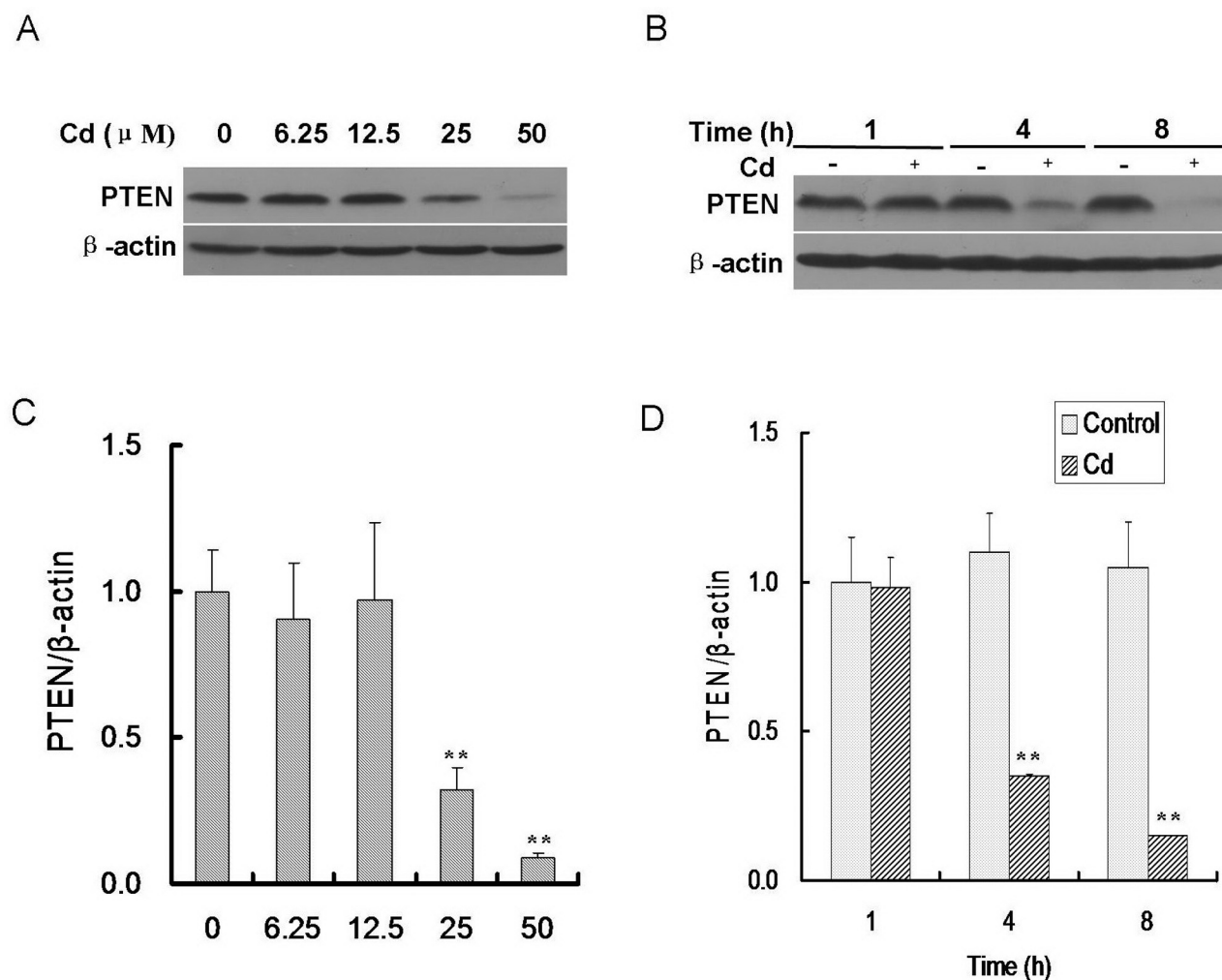


FIG. 4. Cd^{2+} reduces the level of PTEN protein in rodent macrophages. (A) and (C) RAW264.7 cells were incubated with different concentrations of CdCl_2 (0, 6.25, 12.5, 25, and 50.0 μM). PTEN protein was measured using Western blot at 8 h after CdCl_2 . (B) and (D) RAW264.7 cells were incubated with CdCl_2 (50.0 μM). PTEN protein was measured using Western blot at 1, 4, and 8 h after CdCl_2 . Data were expressed as means \pm SEM of six samples. ** $P < 0.01$ as compared with control group.

PTEN protein in macrophages in a dose- and time-dependent manner. Of interest, pretreatment with MG132, a specific proteasome inhibitor, completely blocked Cd^{2+} -evoked reduction in PTEN protein. Correspondingly, MG132 significantly attenuated Cd^{2+} -induced Akt phosphorylation in macrophages. These results suggest that proteasome-mediated PTEN degradation is involved in Cd^{2+} -induced Akt phosphorylation in macrophages.

The present study also observed a slight downregulation of PTEN mRNA in Cd^{2+} -treated macrophages. However, the contribution of decreased PTEN mRNA appears to be minimal in Cd^{2+} -induced reduction in PTEN protein for the following reasons: first, PTEN protein is decreased by 90% in Cd^{2+} -treated macrophages, whereas treatment with Cd^{2+} only causes a slight reduction in PTEN mRNA; second, the reduction in PTEN protein occurs earlier than the downregulation of PTEN mRNA

in Cd^{2+} -stimulated macrophages. Several studies reported that polyubiquitination of PTEN led to its degradation, during which the ubiquitin ligase Nedd4-1 was dispensable for the regulation of PTEN stability and localization (Fouladkou *et al.*, 2008; Trotman *et al.*, 2007; Wang and Jiang, 2008). According to a recent study, PTEN is also post-translationally modified by the small ubiquitin-like proteins, small ubiquitin-related modifier 1 (SUMO1) and SUMO2 (Gonzalez-Santamaria *et al.*, 2012). Indeed, several studies showed that Cd^{2+} elevated accumulation of high-molecular weight of polyubiquitinated proteins in mouse embryonic fibroblast cells and primary rat Sertoli cell-gonocyte cocultures (Yu *et al.*, 2008, 2011). The present study found for the first time that Cd^{2+} exposure induced ubiquitination of PTEN protein in macrophages in a dose-dependent manner. Further analysis showed that ubiquitinated PTEN protein was partially degraded in Cd^{2+} -stimulated macrophages.

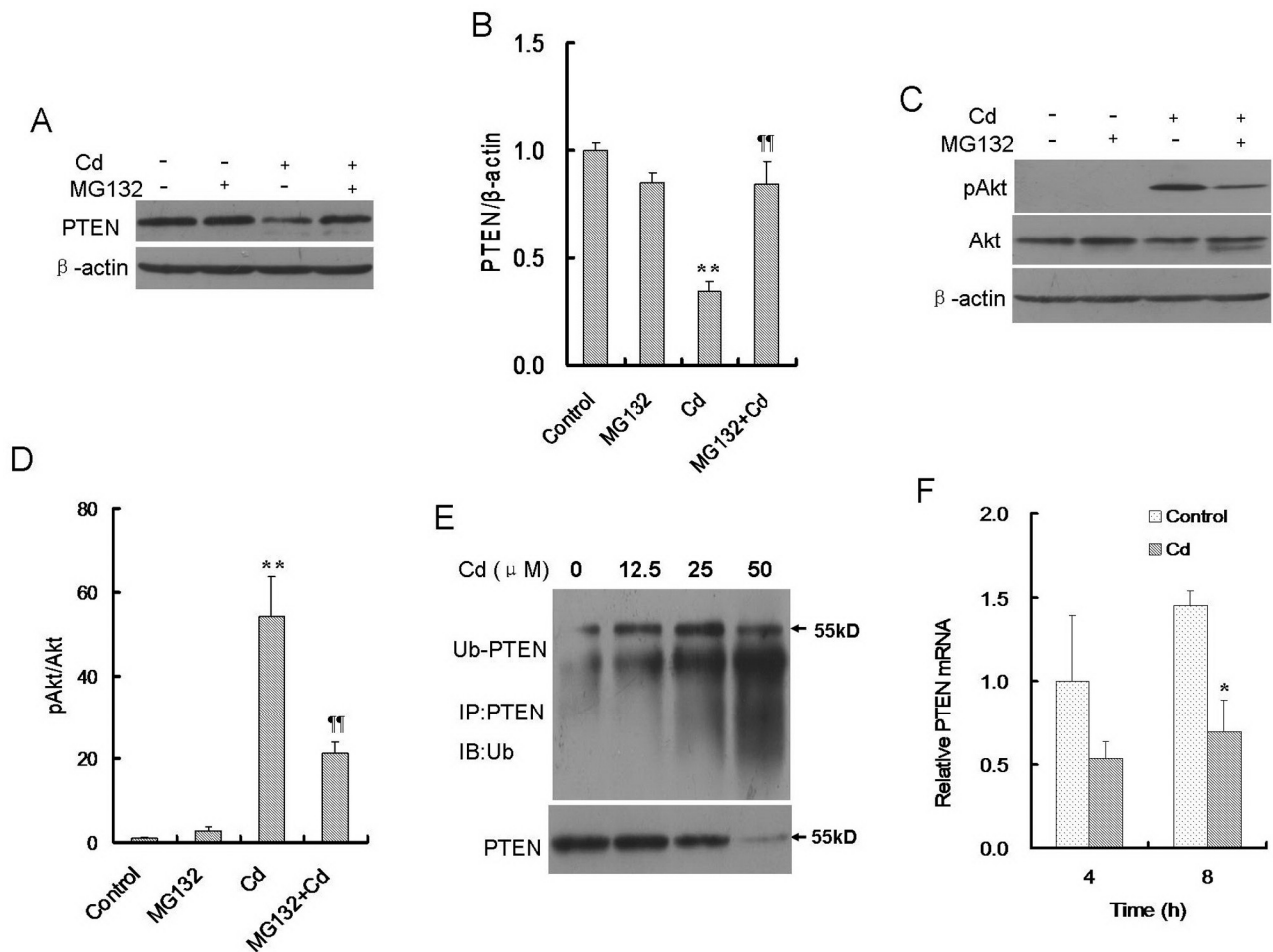


FIG. 5. PTEN ubiquitination mediates Cd²⁺-induced Akt activation in rodent macrophages. (A) RAW264.7 cells were incubated with different concentrations of CdCl₂ (0, 6.25, 12.5, 25, and 50.0 μ M). PTEN ubiquitination was measured using IP at 8 h after CdCl₂. (B)–(E) RAW264.7 cells were incubated with CdCl₂ (50.0 μ M) in the absence or presence of MG132 (50.0 μ M). PTEN, Akt, and pAkt were measured using Western blot at 8 h after CdCl₂. (F) RAW264.7 cells were incubated with CdCl₂ (50.0 μ M). PTEN mRNA was measured using real-time RT-PCR. Data were expressed as means \pm SEM of six samples. **P* < 0.05 and ***P* < 0.01 as compared with control group. ¶¶*P* < 0.01 as compared with CdCl₂ group.

Thus, we guess that PTEN ubiquitination is required for Cd²⁺-induced PTEN degradation in macrophages.

Increasing evidence demonstrates that the ubiquitin-proteasome pathway (UPP) is governed by cellular redox status (Shang and Taylor, 2011). An earlier study showed that a brief exposure of cells to physiologically relevant levels of H₂O₂ induced a transient increase in the UPP activity and intracellular proteolysis (Shang *et al.*, 1997). On the other hand, the UPP activity is also regulated by cellular GSH content. According to an earlier report, cellular GSH depletion aggravates arsenite-induced accumulation of ubiquitinated proteins in human urothelial cells (Bredfeldt *et al.*, 2004). A recent study found that pretreatment with GSH protected against arsenite-induced protein ubiquitination in γ -glutamate cysteine ligase catalytic subunit (Gclc)-deficient cells (Habib *et al.*, 2007). Indeed, the present study revealed that GSH content

was significantly decreased in Cd²⁺-stimulated macrophages. Moreover, NAC, a GSH precursor, completely blocked Cd²⁺-induced PTEN degradation and Akt phosphorylation in macrophages. By contrast, BSO, a specific inhibitor of GSH synthesis, exacerbated Cd²⁺-induced PTEN degradation and Akt phosphorylation in macrophages. Of interest, the present study revealed that PBN, a free radical scavenger, and vitamin C, a well-known antioxidant, did not protect against Cd²⁺-induced PTEN degradation and Akt phosphorylation in macrophages. Actually, vitamin C exacerbated Cd²⁺-induced PTEN degradation and Akt phosphorylation in macrophages. These results suggest that cellular GSH depletion, rather than excess production of reactive oxygen species, mediates ubiquitin-associated PTEN degradation and subsequent Akt phosphorylation in Cd²⁺-stimulated macrophages.

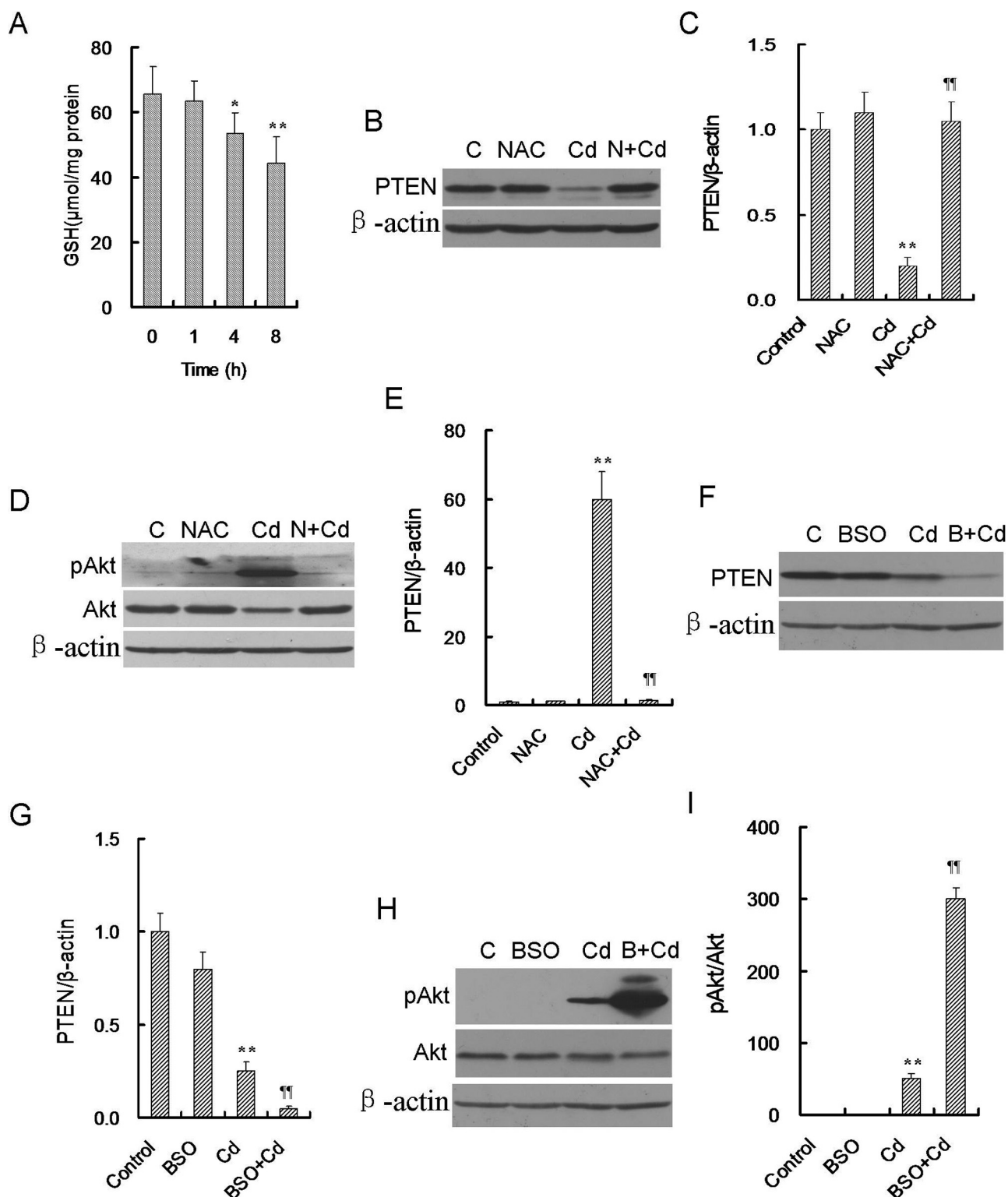


FIG. 6. Differential effects of NAC and BSO on Cd²⁺-induced PTEN reduction and Akt activation in rodent macrophages. (A) RAW264.7 cells were incubated with CdCl₂ (50.0 μM). GSH was measured at 1, 4, and 8 h after CdCl₂. (B)–(E) RAW264.7 cells were incubated with CdCl₂ (50.0 μM) in the absence or presence of NAC (4.0 mM). (B) and (C) PTEN protein was measured using Western blot at 8 h after CdCl₂. (D) and (E) Akt and pAkt were measured using Western blot at 8 h after CdCl₂. (F)–(I) RAW264.7 cells were incubated with CdCl₂ (50.0 μM) in the absence or presence of BSO (1.0 mM). (F) and (G) PTEN protein was measured using Western blot at 8 h after CdCl₂. (H) and (I) Akt and pAkt were measured using Western blot at 8 h after CdCl₂. **P* < 0.05 and ***P* < 0.01 as compared with control group. ***P* < 0.01 as compared with CdCl₂ group.

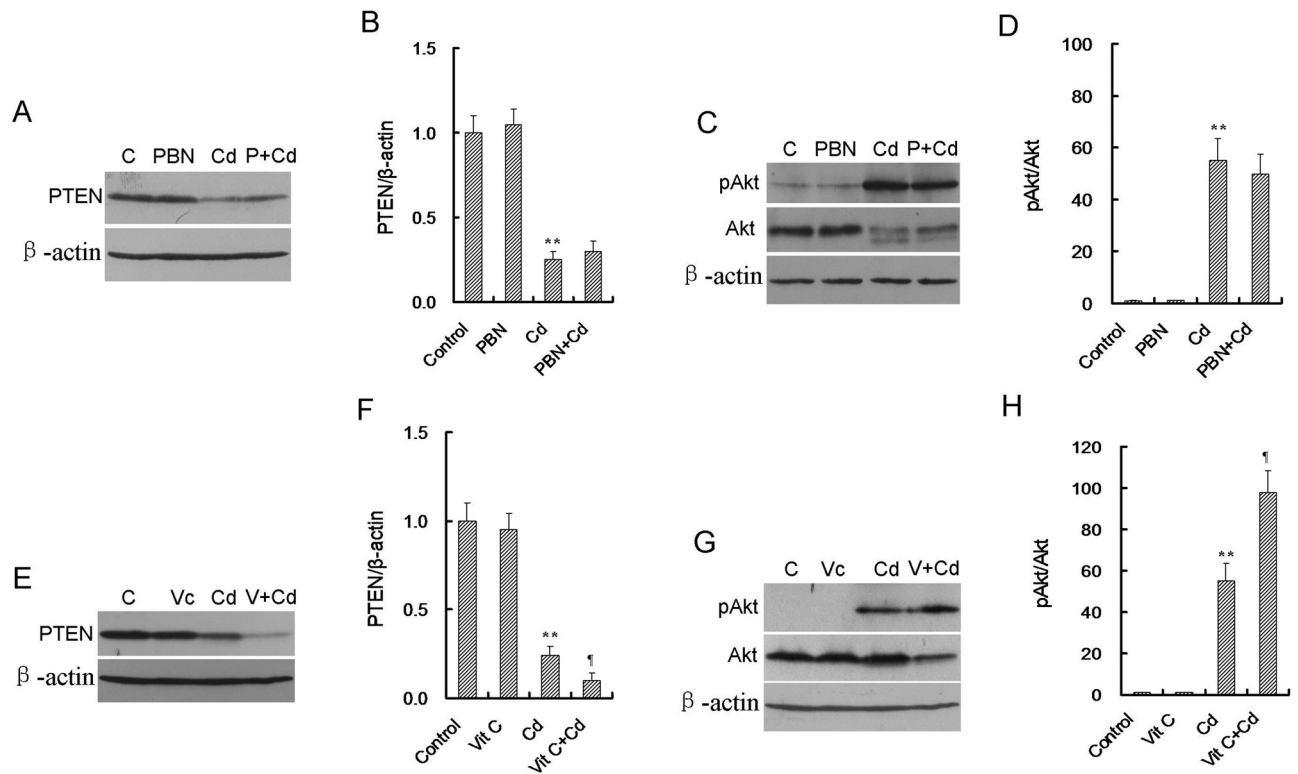


FIG. 7. Effects of PBN and vitamin C on Cd²⁺-induced PTEN reduction and Akt activation in rodent macrophages. (A)–(D) RAW264.7 cells were incubated with CdCl₂ (50.0μM) in the absence or presence of PBN (4.0mM). (A) and (B) PTEN protein was measured using Western blot at 8 h after CdCl₂. (C) and (D) Akt and pAkt were measured using Western blot at 8 h after CdCl₂. (E)–(H) RAW264.7 cells were incubated with CdCl₂ (50.0μM) in the absence or presence of vitamin C (100.0μM). (E) and (F) PTEN protein was measured using Western blot at 8 h after CdCl₂. (G) and (H) Akt and pAkt were measured using Western blot at 8 h after CdCl₂. ***P* < 0.01 as compared with control group. †*P* < 0.05 as compared with CdCl₂ group.

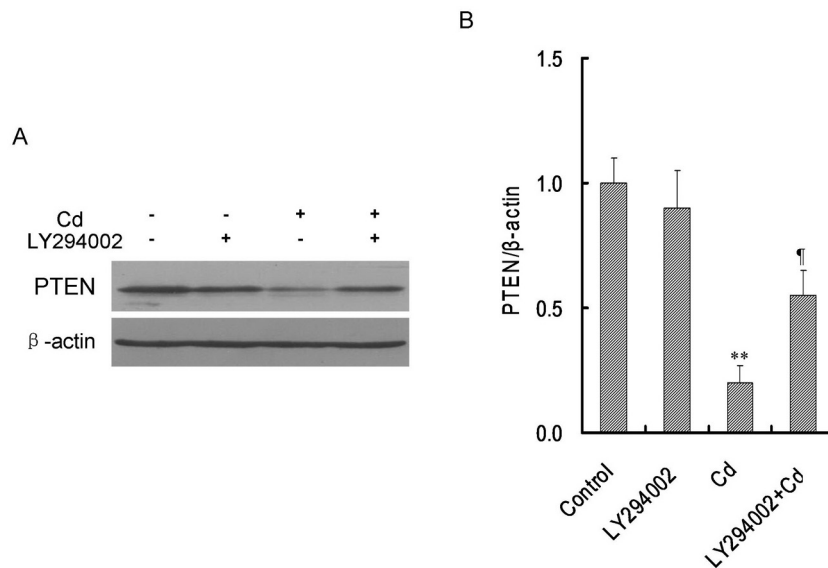


FIG. 8. PI3K Inhibitor partially inhibits Cd²⁺-induced PTEN degradation in macrophages. RAW264.7 cells were incubated with CdCl₂ (50.0μM) in the absence or presence of LY294002 (50.0μM). (A) PTEN protein was measured using Western blot at 8 h after CdCl₂. (B) Data were expressed as means ± SEM of six samples. ***P* < 0.01 as compared with control group. †*P* < 0.05 as compared with CdCl₂ group.

Given that the phosphorylation of PTEN regulates its stability (Leslie *et al.*, 2008), the present study examined the possible role of PI3K/Akt signaling in Cd²⁺-induced degradation of PTEN using a specific PI3K inhibitor, LY294002. Surprisingly, LY294002 partially attenuated Cd²⁺-induced reduction of PTEN in macrophages. These results are in agreement with an earlier report, in which LY294002 significantly attenuated Zn²⁺-induced reduction of PTEN in human airway epithelial cells (Wu *et al.*, 2003). Thus, the present study does not exclude the role of PI3K/Akt signaling in Cd²⁺-induced degradation of PTEN in macrophages.

In summary, the present study indicates that Cd²⁺ selectively upregulates COX-2 and MIP-2 in macrophages in a dose-dependent manner. We demonstrate for the first time that the activation of PI3K/Akt signaling partially contributes to Cd²⁺-induced upregulation of MIP-2 and COX-2 in macrophages. Moreover, proteasome-mediated PTEN degradation is involved in Cd²⁺-induced activation of PI3K/Akt signaling, during which PTEN ubiquitination may play a major role. Finally, cellular GSH depletion mediates ubiquitin-associated PTEN degradation and subsequent activation of PI3K/Akt signaling in Cd²⁺-stimulated macrophages.

SUPPLEMENTARY DATA

Supplementary data are available online at <http://toxsci.oxfordjournals.org/>.

FUNDING

The project was supported by National Natural Science Foundation of China (30901617, 30901217, 30973544, 81172711, and 81373495).

REFERENCES

- Beveridge, R., Pintos, J., Parent, M. E., Asselin, J., and Siemiatycki, J. (2010). Lung cancer risk associated with occupational exposure to nickel, chromium VI, and cadmium in two population-based case-control studies in Montreal. *Am. J. Ind. Med.* **53**, 476–485.
- Bredfeldt, T. G., Kopplin, M. J., and Gandolfi, A. J. (2004). Effects of arsenite on UROtsa cells: Low-level arsenite causes accumulation of ubiquitinated proteins that is enhanced by reduction in cellular glutathione levels. *Toxicol. Appl. Pharmacol.* **198**, 412–418.
- Byrne, C., Divekar, S. D., Storch, G. B., Parodi, D. A., and Martin, M. B. (2009). Cadmium—A metallothionein? *Toxicol. Appl. Pharmacol.* **238**, 266–271.
- Chen, B. C., Kang, J. C., Lu, Y. T., Hsu, M. J., Liao, C. C., Chiu, W. T., Yeh, F. L., and Lin, C. H. (2009). Rac1 regulates peptidoglycan-induced nuclear factor-kappaB activation and cyclooxygenase-2 expression in RAW 264.7 macrophages by activating the phosphatidylinositol 3-kinase/Akt pathway. *Mol. Immunol.* **46**, 1179–1188.
- Cormet-Boyaka, E., Jolivet, K., Bonnegarde-Bernard, A., Rennolds, J., Hassan, F., Mehta, P., Tridandapani, S., Webster-Marketon, J., and Boyaka, P. N. (2012). An NF-kappaB-independent and Erk1/2-dependent mechanism controls CXCL8/IL-8 responses of airway epithelial cells to cadmium. *Toxicol. Sci.* **125**, 418–429.
- Foster, J. G., Blunt, M. D., Carter, E., and Ward, S. G. (2012). Inhibition of PI3K signaling spurs new therapeutic opportunities in inflammatory/autoimmune diseases and hematological malignancies. *Pharmacol. Rev.* **64**, 1027–1054.
- Fouladkou, F., Landry, T., Kawabe, H., Neeb, A., Lu, C., Brose, N., Stambolic, V., and Rotin, D. (2008). The ubiquitin ligase Nedd4-1 is dispensable for the regulation of PTEN stability and localization. *Proc. Natl. Acad. Sci. U. S. A.* **105**, 8585–8590.
- Gonzalez-Santamaria, J., Campagna, M., Ortega-Molina, A., Marcos-Villar, L., de la Cruz-Herrera, C. F., Gonzalez, D., Gallego, P., Lopitz-Otsoa, F., Esteban, M., Rodriguez, M. S., *et al.* (2012). Regulation of the tumor suppressor PTEN by SUMO. *Cell Death Dis.* **3**, e393.
- Haase, H., Ober-Blobaum, J. L., Engelhardt, G., Hebel, S., and Rink, L. (2010). Cadmium ions induce monocytic production of tumor necrosis factor-alpha by inhibiting mitogen activated protein kinase dephosphorylation. *Toxicol. Lett.* **198**, 152–158.
- Habib, G. M., Shi, Z. Z., and Lieberman, M. W. (2007). Glutathione protects cells against arsenite-induced toxicity. *Free Radic. Biol. Med.* **42**, 191–201.
- Harris, S. J., Parry, R. V., Westwick, J., and Ward, S. G. (2008). Phosphoinositide lipid phosphatases: natural regulators of phosphoinositide 3-kinase signaling in T lymphocytes. *J. Biol. Chem.* **283**, 2465–2469.
- Hollander, M. C., Blumenthal, G. M., and Dennis, P. A. (2011). PTEN loss in the continuum of common cancers, rare syndromes and mouse models. *Nat. Rev. Cancer* **11**, 289–301.
- Hyun, J. S., Satsu, H., and Shimizu, M. (2007). Cadmium induces interleukin-8 production via NF-kappaB activation in the human intestinal epithelial cell, Caco-2. *Cytokine* **37**, 26–34.
- Jing, Y., Liu, L. Z., Jiang, Y., Zhu, Y., Guo, N. L., Barnett, J., Rojanasakul, Y., Agani, F., and Jiang, B. H. (2012). Cadmium increases HIF-1 and VEGF expression through ROS, ERK, and AKT signaling pathways and induces malignant transformation of human bronchial epithelial cells. *Toxicol. Sci.* **125**, 10–19.
- Lag, M., Rodionov, D., Ovrevik, J., Bakke, O., Schwarze, P. E., and Refsnes, M. (2010). Cadmium-induced inflammatory responses in cells relevant for lung toxicity: Expression and release of cytokines in fibroblasts, epithelial cells and macrophages. *Toxicol. Lett.* **193**, 252–260.
- Lee, K. S., Kim, S. R., Park, S. J., Lee, H. K., Park, H. S., Min, K. H., Jin, S. M., and Lee, Y. C. (2006). Phosphatase and tensin homolog deleted on chromosome 10 (PTEN) reduces vascular endothelial growth factor expression in allergen-induced airway inflammation. *Mol. Pharmacol.* **69**, 1829–1839.
- Leslie, N. R., Batty, I. H., Maccario, H., Davidson, L., and Downes, C. P. (2008). Understanding PTEN regulation: PIP2, polarity and protein stability. *Oncogene* **27**, 5464–5476.
- Liu, Z., Yu, X., and Shaikh, Z. A. (2008). Rapid activation of ERK1/2 and AKT in human breast cancer cells by cadmium. *Toxicol. Appl. Pharmacol.* **228**, 286–294.
- Miller, Y. I., Viriyakosol, S., Worrall, D. S., Boullier, A., Butler, S., and Witztum, J. L. (2005). Toll-like receptor 4-dependent and -independent cytokine secretion induced by minimally oxidized low-density lipoprotein in macrophages. *Arterioscler. Thromb. Vasc. Biol.* **25**, 1213–1219.
- Miyahara, T., Katoh, T., Watanabe, M., Mikami, Y., Uchida, S., Hosoe, M., Sakuma, T., Nemoto, N., Takayama, K., and Komurasaki, T. (2004). Involvement of mitogen-activated protein kinases and protein kinase C in cadmium-induced prostaglandin E2 production in primary mouse osteoblastic cells. *Toxicology* **200**, 159–167.
- Rodriguez-Barbero, A., Dorado, F., Velasco, S., Pandiella, A., Banas, B., and Lopez-Novoa, J. M. (2006). TGF-beta1 induces COX-2 expression and PGE2 synthesis through MAPK and PI3K pathways in human mesangial cells. *Kidney Int.* **70**, 901–909.

- Romare, A., and Lundholm, C. E. (1999). Cadmium-induced calcium release and prostaglandin E2 production in neonatal mouse calvaria are dependent on cox-2 induction and protein kinase C activation. *Arch. Toxicol.* **73**, 223–228.
- Seok, S. M., Park, D. H., Kim, Y. C., Moon, C. H., Jung, Y. S., Baik, E. J., Moon, C. K., and Lee, S. H. (2006). COX-2 is associated with cadmium-induced ICAM-1 expression in cerebrovascular endothelial cells. *Toxicol. Lett.* **165**, 212–220.
- Shang, F., Gong, X., and Taylor, A. (1997). Activity of ubiquitin-dependent pathway in response to oxidative stress. Ubiquitin-activating enzyme is transiently up-regulated. *J. Biol. Chem.* **272**, 23086–23093.
- Shang, F., and Taylor, A. (2011). Ubiquitin-proteasome pathway and cellular responses to oxidative stress. *Free Radic. Biol. Med.* **51**, 5–16.
- Son, Y. O., Wang, L., Poyil, P., Budhraj, A., Hitron, J. A., Zhang, Z., Lee, J. C., and Shi, X. (2012). Cadmium induces carcinogenesis in BEAS-2B cells through ROS-dependent activation of PI3K/AKT/GSK-3beta/beta-catenin signaling. *Toxicol. Appl. Pharmacol.* **264**, 153–160.
- Song, M. S., Salmena, L., and Pandolfi, P. P. (2012). The functions and regulation of the PTEN tumour suppressor. *Nat. Rev. Mol. Cell Biol.* **13**, 283–296.
- Suzuki, A., Yamaguchi, M. T., Ohteki, T., Sasaki, T., Kaisho, T., Kimura, Y., Yoshida, R., Wakeham, A., Higuchi, T., Fukumoto, M., *et al.* (2001). T cell-specific loss of Pten leads to defects in central and peripheral tolerance. *Immunity* **14**, 523–534.
- Trotman, L. C., Wang, X., Alimonti, A., Chen, Z., Teruya-Feldstein, J., Yang, H., Pavletich, N. P., Carver, B. S., Cordon-Cardo, C., Erdjument-Bromage, H., *et al.* (2007). Ubiquitination regulates PTEN nuclear import and tumor suppression. *Cell* **128**, 141–156.
- Wang, X., and Jiang, X. (2008). Post-translational regulation of PTEN. *Oncogene* **27**, 5454–5463.
- Wu, W., Wang, X., Zhang, W., Reed, W., Samet, J. M., Whang, Y. E., and Ghio, A. J. (2003). Zinc-induced PTEN protein degradation through the proteasome pathway in human airway epithelial cells. *J. Biol. Chem.* **278**, 28258–28263.
- Yu, X., Hong, S., and Faustman, E. M. (2008). Cadmium-induced activation of stress signaling pathways, disruption of ubiquitin-dependent protein degradation and apoptosis in primary rat Sertoli cell-gonocyte cocultures. *Toxicol. Sci.* **104**, 385–396.
- Yu, X., Sidhu, J. S., Hong, S., Robinson, J. F., Ponce, R. A., and Faustman, E. M. (2011). Cadmium induced p53-dependent activation of stress signaling, accumulation of ubiquitinated proteins, and apoptosis in mouse embryonic fibroblast cells. *Toxicol. Sci.* **120**, 403–412.
- Zhao, Z., Hyun, J. S., Satsu, H., Kakuta, S., and Shimizu, M. (2006). Oral exposure to cadmium chloride triggers an acute inflammatory response in the intestines of mice, initiated by the over-expression of tissue macrophage inflammatory protein-2 mRNA. *Toxicol. Lett.* **164**, 144–154.